The Astrophysical Journal, 649:490–497, 2006 September 20

RAPID CHANGES OF PHOTOSPHERIC MAGNETIC FIELDS AROUND FLARING MAGNETIC NEUTRAL LINES

Haimin Wang
Big Bear Solar Observatory, New Jersey Institute of Technology, 40386 North Shore Lane,
Big Bear City, CA 92314-9672; haimin@flare.njit.edu
Received 2006 May 5; accepted 2006 May 30

ABSTRACT

In this paper we study the short-term evolution of magnetic fields associated with five flares in δ-sunspots. We concentrate on the analysis of the magnetic gradient along the flaring neutral lines (NLs). Obvious changes of the magnetic gradient occurred immediately and rapidly following the onset of each flare. A rapid gradient increase was found to be associated with three events, while a decrease was associated with the other two. The changes were permanent, and therefore not likely due to the flare emissions. In addition, we evaluated the mean relative motions between the two magnetic polarities in these δ-regions, in the directions parallel and perpendicular to the flaring NLs. We derived the mean positions of the two magnetic polarities using a center-of-mass (CoM) calculation and found that (1) converging motions correspond to a gradient increase and diverging motions, to a decrease; (2) for all the events, there appeared a sudden release of magnetic shear associated with each flare, signified by a decrease of CoM separation between 500 and 1200 km in the direction parallel to the NLs. Combining the findings presented here with those in previous papers, we propose that these results are evidence of magnetic reconnection at or close to the photosphere. When an active region is away from the solar disk center, the reconnected transverse fields cause an apparent increase of the flux in the polarity toward the limb and a decrease for the polarity closer to the disk center. This observational pattern was indeed found for all 10 available events that have been studied in the literature and in this paper. Finally, we offer some predictions for future observations when high-quality vector magnetogram sequences become available.

Subject headings: Sun: activity — Sun: coronal mass ejections (CMEs) — Sun: flares — Sun: magnetic fields

1. INTRODUCTION

Only recently have rapid and permanent changes of photospheric magnetic fields been observed to be associated with large solar flares. Over a decade ago, the Big Bear Solar Observatory (BBSO) group discovered rapid and permanent changes of vector magnetic fields associated with flares (Wang et al. 1992, 1994), but several other studies generated inconclusive results (Ambastha et al. 1993; Hagyard et al. 1999; Chen et al. 1994; Li et al. 2000a, 2000b). Kosovichev & Zharkova (2001) studied high-resolution Michelson Doppler Imager (MDI) magnetogram data for the 2000 July 14 "Bastille Day Flare" and found regions with a permanent decrease of the magnetic flux, which was related to the release of magnetic energy. Using 1 minute cadence GONG++ data, Sudol & Harvey (2005) observed rapid and permanent changes of line-of-sight magnetic fields that were indeed associated with almost all the X-class flares studied. Earlier, the BBSO group published a number of papers describing the sudden appearance of unbalanced magnetic flux that is associated with flares (Spirock et al. 2002; Wang et al. 2002b, 2004b; Yurchyshyn et al. 2004).

Very recently, the BBSO group presented a new observational result of the rapid changes of sunspot structure associated with a substantial fraction of flares (Wang et al. 2004a; Deng et al. 2005; Liu et al. 2005; Chen et al. 2006). In particular, Liu et al. (2005) studied the change in δ-spot structures associated with seven X-class flares. The results are quite consistent for all the events: part of the penumbral segments in the outer δ-spot structure decay rapidly after major flares, and meanwhile, the neighboring umbral cores and/or inner penumbral regions become darker. The rapid changes, which can be identified in the time profiles of the white-light mean intensity, are permanent, not transient, and thus are not due to flare emissions. The co-aligned magnetic field observations show substantial changes in the longitudinal magnetic field associated with the decaying penumbrae and darkened central areas. For two events in which the vector magnetograms were available, Liu et al. (2005) found that the transverse fields associated with the penumbral decay areas decreased, while they increased at the flare neutral lines (NLs). Both events also showed an increase in the photospheric magnetic shear after the flares. For all the events, they found that the locations of penumbral decay were related to flare emissions and were connected by prominent *Transition Region and Coronal Explorer* (*TRACE*) postflare loops. To explain these observations, they proposed a reconnection picture in which the two components of a δ-spot become strongly connected after the flare. In the outer border of the δ-structure, the penumbral fields change from a highly inclined to a more vertical configuration, which leads to penumbral decay. The umbral core and inner penumbral region close to a NL become darker as a result of increased field strength there, mainly in the form of transverse fields.

Measurements of the nonpotentiality of an active region can be obtained from a vector magnetogram of the region. These measurements can be used as a proxy to predict the time and location of flares. Study of the evolution of these parameters would further provide information about energy storage and release during the process of flares. Zhang (2001) found that the shear and gradient of the magnetic field are important in defining the nonpotentiality of solar active regions and that they reflect the strength of the electric current in the regions. However, the analysis of vector magnetograms has experienced difficulties even as new instruments have been developed. The most notable ones are calibration,

TABLE 1
PROPERTIES OF FIVE FLARES AND THE ASSOCIATED ACTIVE REGIONS

Date	Flare Time (UT)	Flare Magnitude	NOAA Region	Latitude (deg)	Longitude (deg)
2001 Apr 6..........	19:13	X5.6	9415	S21	E30
2001 Apr 9..........	15:25	M7.9	9415	S21	E19
2003 Oct 28.........	11:10	X17	10486	S16	E08
2003 Oct 29.........	16:31	X10	10486	S16	W08
2005 Sep 13.........	19:27	X1.2	10808	S09	E10

resolution of 180° ambiguity, and correction of the projection effect when an observed region is not close to the solar disk center. From a sample of 17 vector magnetograms, Falconer et al. (2003) showed that there is a viable proxy for nonpotentiality that can be measured from a line-of-sight magnetogram. This proxy is the strong magnetic gradient, and it is correlated with active region coronal mass ejection (CME) productivity. Because gradients can be measured from line-of-sight magnetograms obtained from conventional magnetographs, they may be a dependable substitute for magnetic shear for use in operational flare and CME forecasting. Prasad (2000) used the similar parameter of the magnetic gradient to characterize the stressed magnetic fields in active regions. Wang et al. (2006) found a close correlation between magnetic shear and magnetic gradient; both can be used as a good proxy to predict flares. This was further demonstrated by statistical studies (Song et al. 2006; Jing et al. 2006).

Naturally, we extend the study one step further, i.e., to detect changes of the magnetic gradient in the flaring NLs and the relative motion between the two opposite magnetic polarities divided by the NLs. This is the primary objective of this paper. In conception, the study is similar to the investigation of earthquakes, studying the stress and motion between two tectonic plates. Preliminary studies for two individual cases can be found in Deng et al. (2006) and Stoltz (2005); both showed some obvious evidence of rapid gradient changes associated with the flares.

2. OBSERVATIONS AND RESULTS

The reliable detection of rapid changes in observed magnetic fields would require stable observing conditions. Therefore, we use MDI line-of-sight magnetograms in this study to take advantage of long-sequence and seeing-free conditions. We only use the data sets that have a cadence of 1 minute. The magnetograms have a pixel resolution of 2″. We select the regions that have data coverage for longer than 10 hr with a large flare (mostly X-class with one exception of M7.9) in the middle. Table 1 lists some basic properties of the five events.

We first describe the 2001 April 9 event as an example to demonstrate the data analysis procedures. This event was studied previously by Yurchyshyn et al. (2006). They demonstrated that this region had a typical sigmoid configuration. Figure 1 shows an MDI magnetogram at 15:00 UT, shortly before the onset of the M7.9 flare. In order to conveniently study the evolution of magnetic fields near the flaring NL and the motion of the fields perpendicular and parallel to the NL, we first rotate each magnetogram so that the NL appears to be in the vertical direction. For the 2001 April 9 event, we rotated 23° clockwise. Based on the Hα movie, we identify the flaring NL, i.e., the dark vertical line in the Hα image. A dark box is drawn to isolate the δ-sunspot where the flare was initiated and to mark the area for the calculations below. The same NL is marked on the calculated gradient map (Fig. 1, *right*). Five parameters were calculated using each magnetogram, and based on these, five time profiles were generated to describe the evolution of magnetic structure with 1 minute cadence. These parameters are (1) negative magnetic flux in the box, (2) positive flux, (3) mean magnetic gradient along the flaring NL, (4) the center-of-mass (CoM) separation of the two magnetic polarities perpendicular to the NL, indicating either convergent or divergent motion, and (5) the CoM separation parallel to the

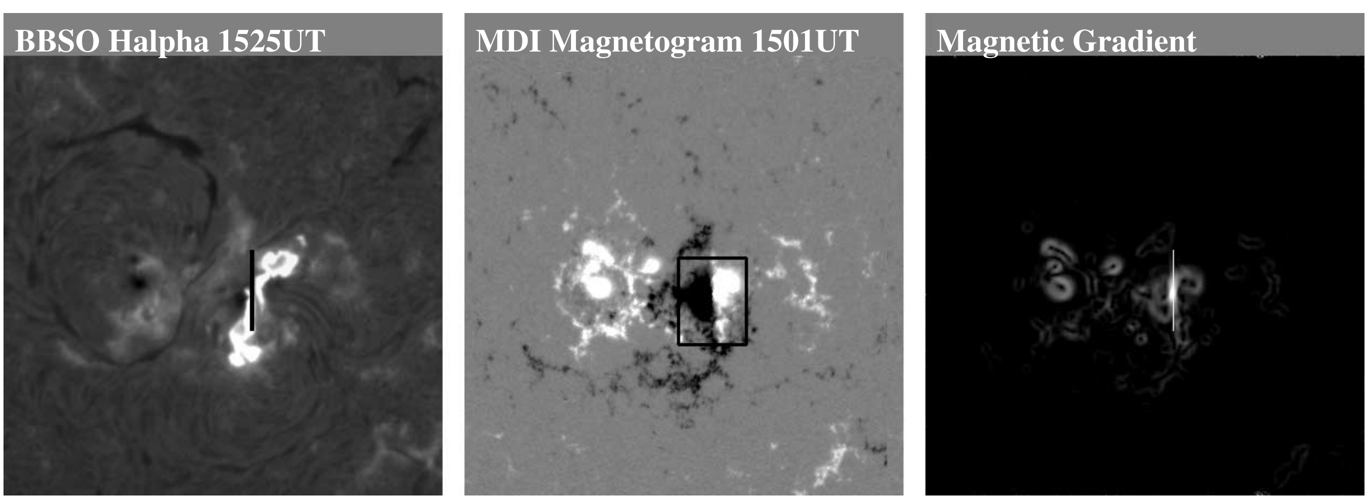

FIG. 1.—*Left:* BBSO Hα image during the 2001 April 9 flare in AR 9415. *Middle:* MDI magnetogram. *Right:* Gradient map derived from magnetogram. The field of view is $400'' \times 400''$. The black box defines the area of magnetic flux and CoM separation calculation. The black vertical line on the left and white vertical line on the right indicate the flaring magnetic NL.

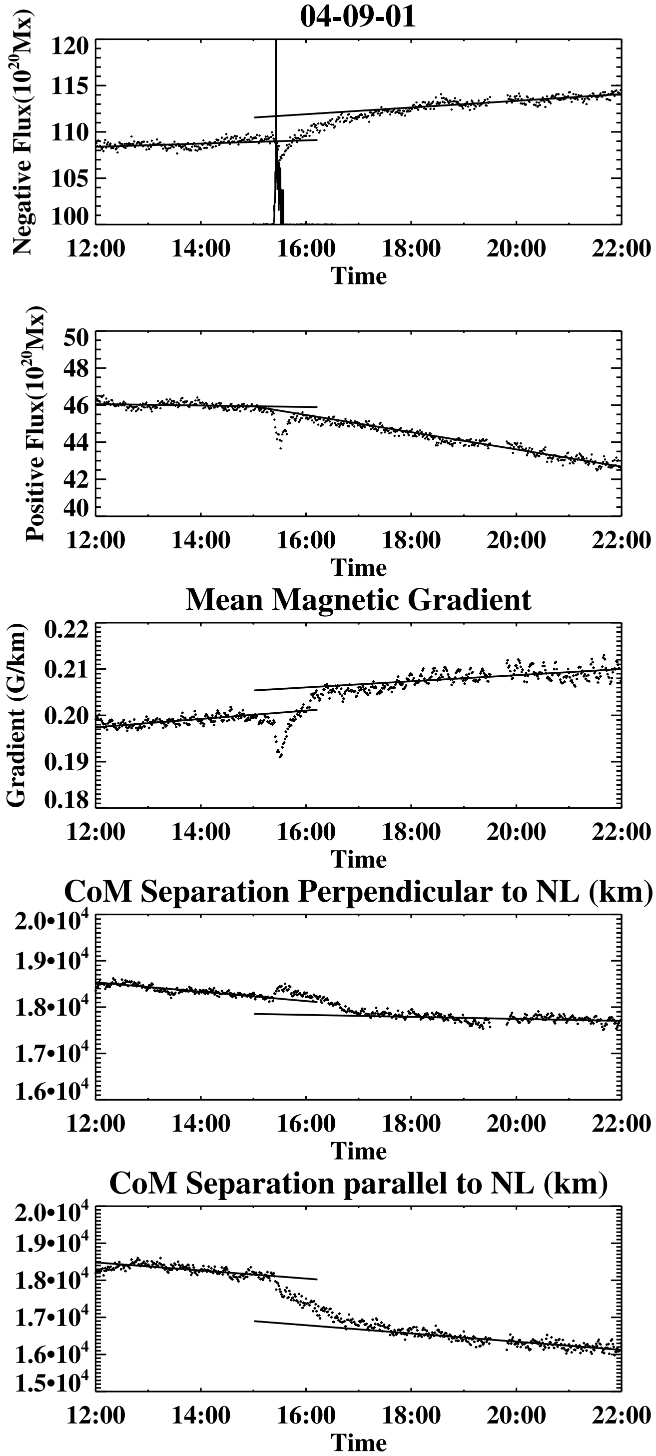

FIG. 2.—Time profiles for the 2001 April 9 event. *Top to bottom:* Negative magnetic flux, positive magnetic flux, mean magnetic gradient along the flaring NL, CoM separation perpendicular to the NL, and CoM separation parallel to the NL. The thin vertical line marks the time of the maximum rate of increase of *GOES* soft X-ray flux.

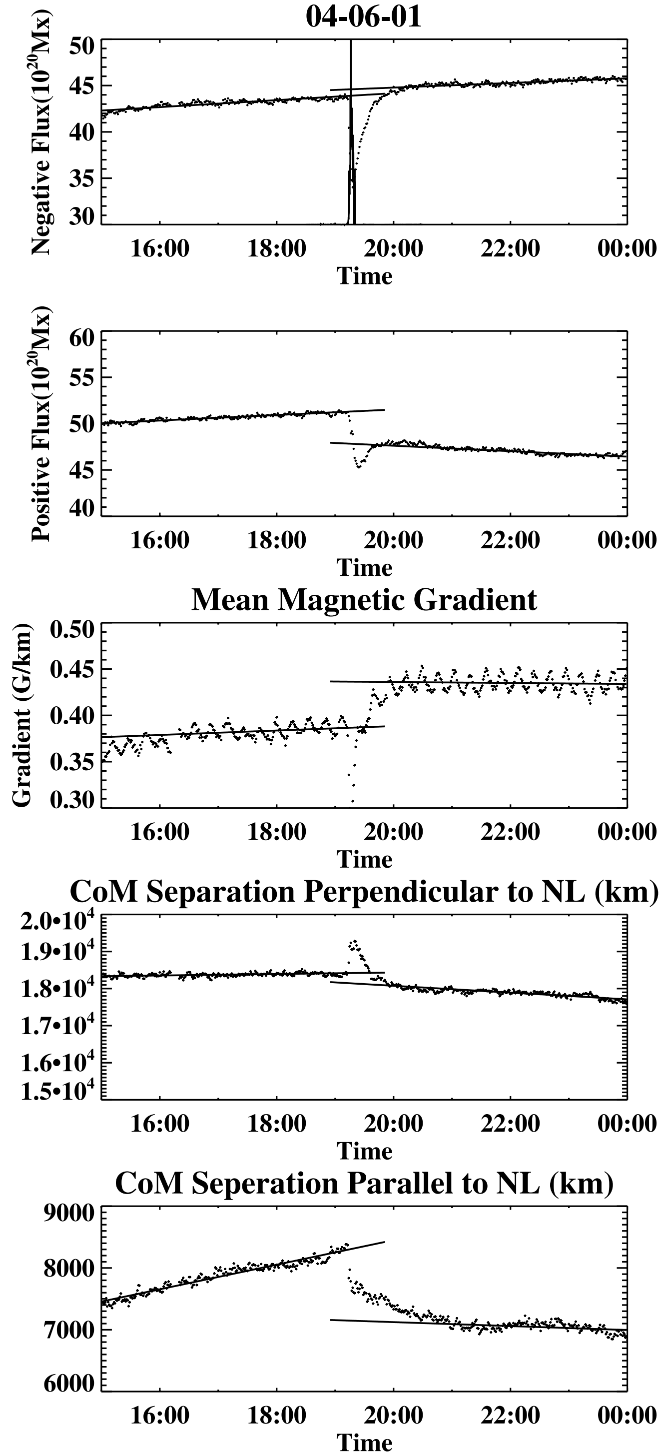

FIG. 3.—Same as Fig. 2, but for the 2001 April 6 event.

NL, indicating the shear motion. The CoM x- and y-positions are defined as

$$X_c = \frac{\sum X_i B_i}{\sum B_i}, \quad Y_c = \frac{\sum Y_i B_i}{\sum B_i},$$

where X_i and Y_i are the x- and y-coordinates of a given point and B_i is the corresponding measured magnetic flux density. If we use all the points with $B_i \geq 0$, the resulting CoM position would be for the positive polarity flux; if we use all the points with $B_i \leq 0$, the resulting CoM position would be for the negative polarity flux. The magnetic gradient was calculated using the code provided by Gallagher et al. (2002).

Visual inspection of time profiles clearly demonstrates sudden changes in the parameters. The changes begin at the time of the flares. To quantitatively describe these changes for each time profile, we divide the data points into two sections: from the beginning of the observation to about a half-hour before the flare and from 2 hr after the flare to the end of the observation.

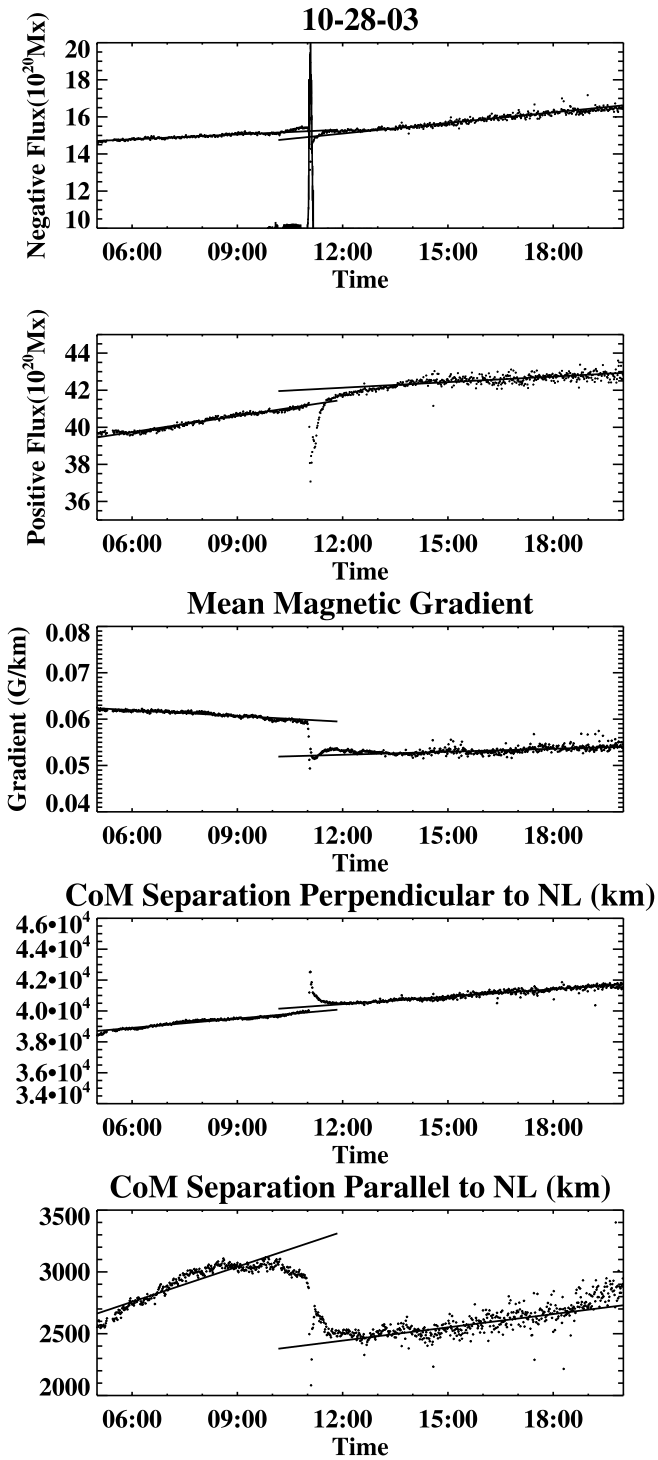

FIG. 4.—Same as Fig. 2, but for the 2003 October 28 event.

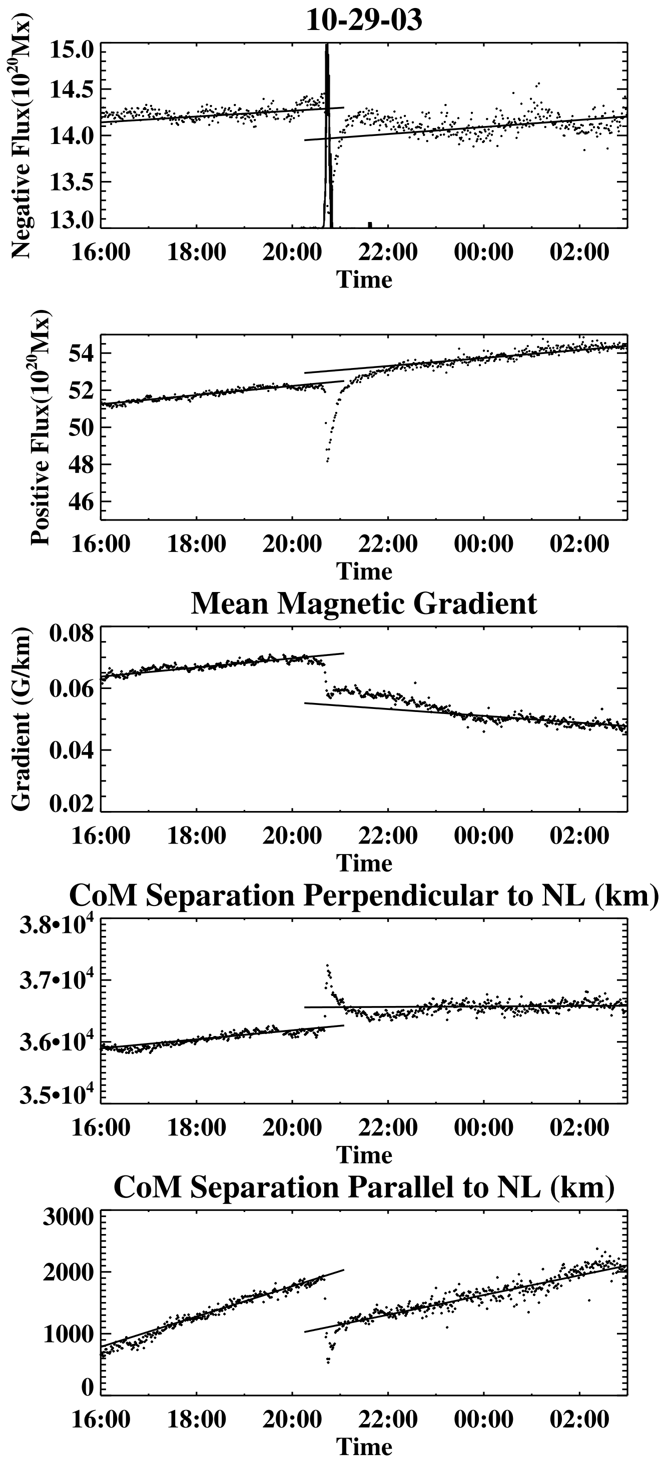

FIG. 5.—Same as Fig. 2, but for the 2003 October 29 event.

Comparison of the linear fittings in these two sections can provide evidence of either a sudden jump of parameters or a change in the trend of magnetic field evolution associated with the flare. We intentionally skipped about 2.5 hr of data covering each flare to avoid possible line profile change during the flare that would likely affect the measured magnetic signal (Qiu & Gary 2003). In this study we are more interested in the discontinuity (signifying the rapid changes) in the parameters around the flare time instead of the long-term evolution of the parameters.

We note that we are only measuring magnetic fields in the coordinates of the plane of the sky, instead of the true heliospheric coordinates. The projection effect would prevent the accurate determination of true longitudinal fields perpendicular to the solar surface. Overcoming this weakness requires high-quality long-sequence vector magnetic field measurements, which are not currently available. Nevertheless, the projection effect will not cause a sudden change in magnetic fields. If there is no intrinsic solar magnetic field change, the largest change of the observed fields would be due to the solar rotation, which cannot create a sudden jump on the timescale of 1 hr.

In Figure 2 we plot the aforementioned time profiles and fittings for the 2001 April 9 event. Figures 3–6 present similar plots for

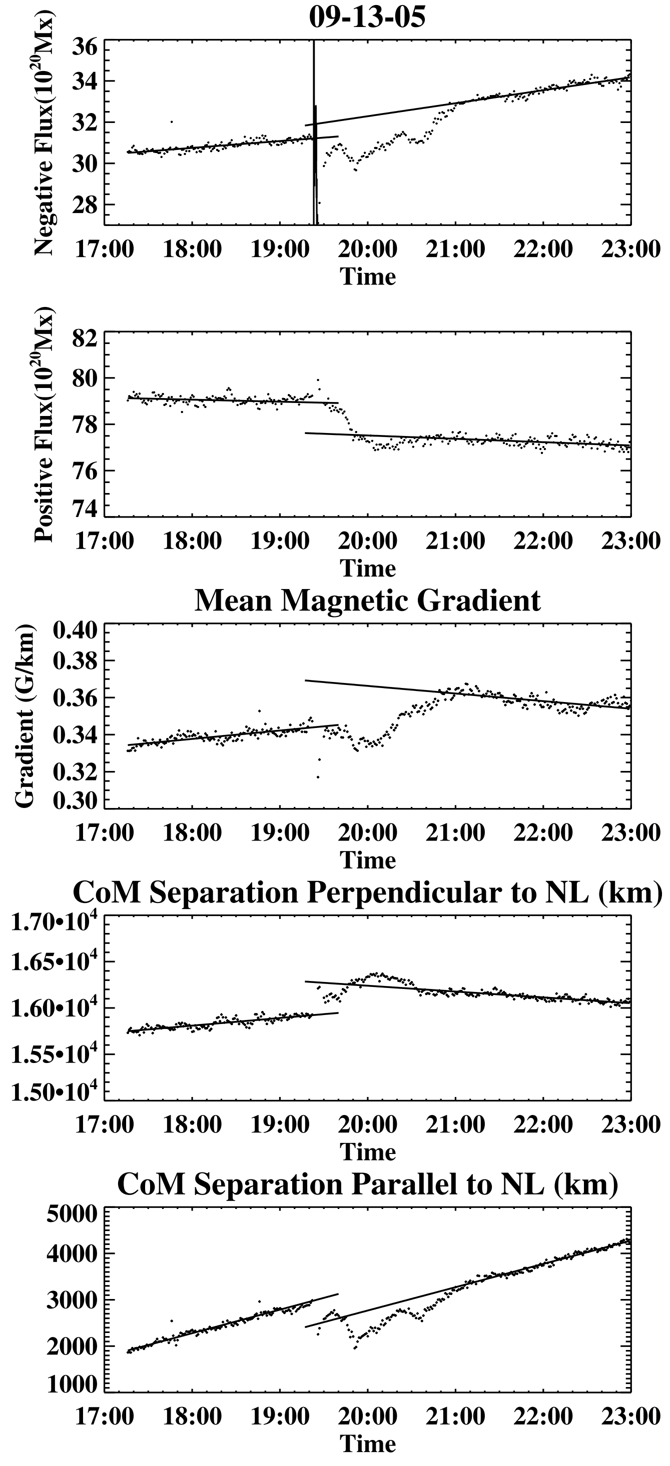

FIG. 6.—Same as Fig. 2, but for the 2005 September 13 event.

the other four events. Table 2 lists the summary of changes of the discussed parameters. Following each parameter, we describe the trends of the parameters. For example, "+/−" would indicate that the parameter has an increasing trend before the flare and decreasing after. A trend that is not obvious is denoted by "0".

Based on Figures 2–6 and Table 2, we discuss some common properties of these five events:

1. Without ambiguity, all the parameters have sudden jumps immediately following the onset of the flares. This agrees with the conclusions of previous work that the photospheric fields only change after the start of flares (Wang et al. 2002b; Sudol & Harvey 2005). As we presented, these changes are observed for all the parameters: magnetic flux, magnetic gradient along the flare NLs, and CoM separation between opposite polarities. Again, all these changes are permanent.

2. Unbalanced magnetic flux changes are found for all the events: the flux of one polarity increases while the opposite polarity decreases. This is in agreement with the findings of Wang et al. (2002b). There is only one overlapping event in these two sets of events (this paper and Wang et al. 2002b), i.e., the 2001 April 6 flare.

3. The mean magnetic gradient along the flaring NLs increases for three events and decreases for the other two. For the events with increased gradient, converging motion was evident based on the CoM separation perpendicular to the NL. For the 2001 April 6 flare, the CoM separation decreased by 350 km, and obvious converging motion started following the flare; for the 2001 April 9 flare, CoM separation also decreased by 350 km, and converging motion continued after the flare; for the 2005 September 13 flare, although CoM separation increased by 310 km, the motion changed from diverging to converging following the flare. For the two events (2003 October 28 and 29) for which the gradient decreased, both showed continued diverging motion after the flare and a jump of CoM separation by 380 and 290 km, respectively.

4. The most striking result is the change of CoM separation in the direction parallel to the flaring NL. A decrease of the value represents a decrease of shear. This is the first evidence that the relative shear of the δ-structure decreases suddenly by an amount between 500 and 1200 km for all five events. Please note that the magnitude of the CoM separation change is less than 1 MDI pixel size; it is meaningful only because the result is the average of thousands of data points.

3. DISCUSSIONS

Based on the findings discussed in this paper and combining them with the results in previous papers, we discuss some possible physical insights:

It has been pointed out recently that two-stage reconnection may be responsible for flares and CMEs; a representative model is tether cutting via implosive/explosive connection in the middle of a sigmoid (Moore et al. 2001 and references therein). The first stage is the reconnection near the solar surface, forming an erupting rope. The second stage involves the interaction between the erupting rope and the larger scale arcade fields. We believe that our observations explain the first step of reconnection by the following arguments:

A simplified magnetic topology of this kind of reconnection process was presented by Liu et al. (2005). We now present a modified version in Figure 7 as the cartoon in the left panel. Again, using the 2001 April 9 event as an example, we propose that the flare is the result of the core field reconnection of the sigmoid configuration. The three-dimensional picture of this event was described in more detail by Yurchyshyn et al. (2006). For simplicity, we project this to two dimensions. Before the reconnection, the fields are dominated by the longitudinal component as there is no connectivity between the two poles across the neutral line (NL). After the reconnection slightly above the photosphere, magnetic tension may pull the shorter loop down to the level of the photosphere. Effectively, longitudinal fields would be converted into transverse fields. If the region is at the disk center, this would just be shown as the sudden disappearance of magnetic fields in both polarities due to submergence as discussed by Zwaan (1987). This kind of fast magnetic cancellation

TABLE 2

MAGNETIC PARAMETERS AND THEIR CHANGES

Date	Change of Negative Flux (10^{20} Mx)	Trend of Negative Flux	Change of Positive Flux (10^{20} Mx)	Trend of Positive Flux	Change of Magnetic Gradient (G km^{-1})	Trend of Magnetic Gradient	Change of CoM Perpend. to NL (km)	Trend of CoM Perpend. to NL	Change of CoM Parallel to NL (km)	Trend of CoM Parallel to NL
2001 Apr 6............	+0.85	+/+	−3.4	+/−	+0.057	0/−	−350	+/−	−900	+/−
2001 Apr 9............	+2.7	0/+	0	0/−	+0.005	+/+	−350	−/0	−1200	−/−
2003 Oct 28...........	−0.4	+/+	+0.75	+/+	−0.0075	−/0	+380	+/+	−840	+/+
2003 Oct 29...........	−0.33	+/+	+0.65	+/+	−0.017	+/−	+290	+/0	−890	+/+
2005 Sep 13...........	+0.75	+/+	−1.2	−/−	+0.026	+/−	+310	+/−	−520	+/+

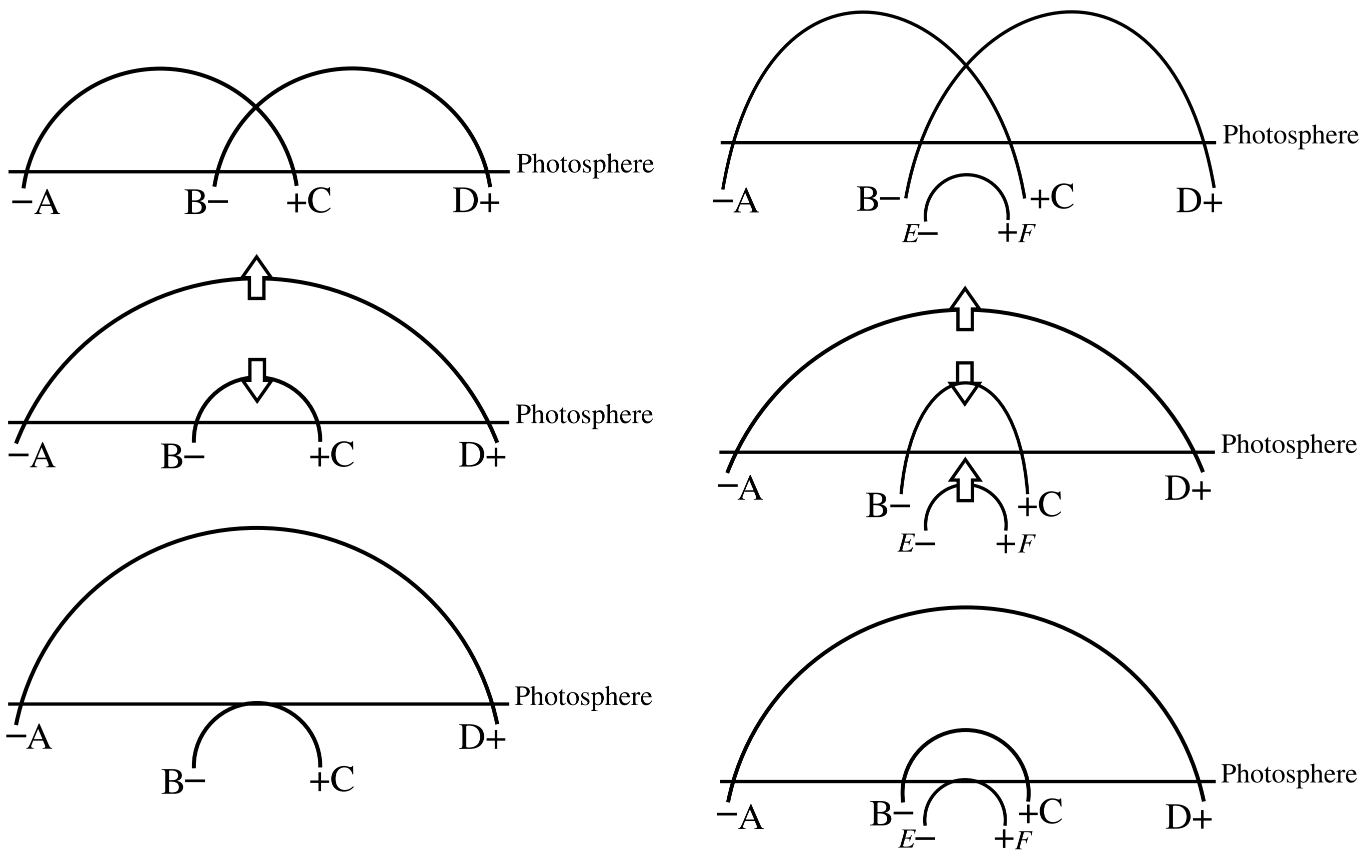

FIG. 7.—Cartoons to explain observations. *Left:* Reconnection and submergence explain the converging motion with an increase of the magnetic gradient at the flaring NL. The crossing of field lines before the reconnection reflects the three-dimensional sigmoid configuration. *Right:* New flux emergence, explaining the divergence and gradient decrease. In either case, the new magnetic connectivity in the photosphere after the flare would cause an increase of transverse fields.

has been occasionally observed (Wang et al. 2002b). If the region is substantially away from the disk center, we are seeing a projected part of the transverse field into the line-of-sight direction as observed by MDI magnetograms. As Spirock et al. (2002) pointed out by a cartoon in Figure 4 of their paper, the flux closer to the limb is enhanced, while that closer to disk center is reduced, if the newly formed transverse field is flat enough. This model can explain the observations of 2001 April 6 and 9 and 2005 September 13, as we observe the converging motion and rapid increase of the magnetic gradient at the NL immediately following the flares.

The cases of 2003 October 28 and 29 are more difficult to explain. We propose a modified scenario: that the sigmoid core field reconnection somehow simplified the field above the solar photosphere, and a new flux emerged as a consequence of this relaxation. The same argument of unbalanced magnetic field evolution still holds as long as the emerged flux loop is flat at the part intersecting the photosphere. The new flux emergence explains the divergent motion and gradient decrease following flares. As a matter of fact, the general trend is that the active region was still in the growing stage during the period of these two events.

If the unbalanced flux evolution is due to the vertically dominated fields switching to horizontally dominated fields, then we should see the effect stated by Spirock et al. (2002), the limbward flux increases while diskward flux decreases. Summarizing all 10 available events from the literature and this paper, we indeed observe such a trend. We only select the events for which the flaring NL is well defined and close to parallel to the limb (less than 30° in angular separation). Table 3 lists the rapid magnetic flux changes after the flares for these events. It is quite evident that for all the events, limbward flux increases, and diskward flux decreases (no apparent change in one event). The probability of random occurrence this way is only 0.1%.

Please note that this first step of reconnection does not release a substantial amount of energy; instead, it changes the magnetic topology for further energy release in the second step. The discussion of the second step is beyond the scope of this paper. It may be part of the breakout process (Antiochos 1998; Antiochos et al. 1999) or may also fit into the classical picture of the Kopp-Pneuman (Kopp & Pneuman 1976) model. The signature of the second step reconnection includes large-scale dimming and remote Hα ribbons (Wang et al. 2002a, 2005; Manoharan et al. 1996), as well as inverse type III bursts (Tang & Moore 1982).

Based on our observations and proposed two-step reconnection picture, we make some predictions for future observations, when high-resolution vector magnetograms will become available, such as from the upcoming space missions *Solar-B* and the *Solar Dynamics Observatory.*

1. Transverse magnetic fields at a flaring NL will increase rapidly following flares. There is some evidence of such an increase (Wang et al. 2002b, 2004b).
2. The unbalanced flux change will be more prominent when the regions are closer to the limb due to the enhanced projection effect there.
3. Evershed flow will decrease in the outer boundary of a δ-configuration, as outward-inclined fields will become more vertical. This was observed in one case (Wang et al. 2005).
4. In the initial phase of the flare (first-stage reconnection), two flare footpoints may move closer before they start the usual

TABLE 3

Limbward and Diskward Flux Changes for 10 Events in the Literature and in This Paper

Date	Limbward Flux (10^{20} Mx)	Diskward Flux (10^{20} Mx)	Reference
1990 May 24........	+	−	Cameron & Sammis (1999)[a]
2001 Apr 2...........	+6	−1.5	Spirock et al. (2002)
2001 Apr 6...........	+4	−4	Wang et al. (2002b)
2001 Apr 9...........	+2.8	0	This paper
2001 Aug 25........	+1.8	−0.4	Wang et al. (2002b)
2001 Oct 22.........	+11	−2	Wang et al. (2002b)
2002 Jul 23..........	+2	−1	Yurchyshyn et al. (2004)
2003 Oct 28.........	+0.75	−0.4	This paper
2003 Oct 29.........	+0.65	−0.33	This paper
2005 Sep 13.........	+0.75	−1.2	This paper

[a] Qualitative results only.

separation motion. The core reconnection may explain such an inward motion: sheared loops are reconnected first and less-sheared loops are reconnected later; therefore, the separation between footpoints may decrease during this phase. The energy balance of this picture can be understood in the context of ''implosion'' as proposed by Hudson (2000). Such early-phase footpoint-converging motion has been observed recently (Ji et al. 2004a, 2004b, 2006; Veronig et al. 2006).

5. In the work of Melrose (1997), he assumes that the reconnected loop systems carry currents. He also predicted that as a consequence of the reconnection, some current will be able to be measured near the photosphere, and therefore, an increase of the magnetic shear near the flaring NLs may be detected. An alternative way to explain this is that the newly emerged fluxes are more strongly sheared. The magnetic shear increase was only observed in a couple of isolated events; therefore, future observations are needed to verify these.

For the last point, we would like to discuss an apparent observational paradox. As we presented in this paper, the overall shear motion has a sudden relaxation after all the events; on the other hand, based on vector magnetograph observations, at the flaring NL, magnetic shear (defined as the difference between the observed vector fields and potential fields) may be observed to increase (Wang et al. 2002b; Liu et al. 2005). We tentatively offer the following explanation: the shear velocity found using the CoM method reflects the overall structure of the active regions, and the shear release reflects the overall energy release; however, the shear increase near the NL is localized, reflecting magnetic connectivity for a small area, and therefore does not provide information about the stored magnetic energy of the active regions.

I would like to express my gratitude to the referee for valuable comments. I thank Chang Liu for helpful discussions, reading the manuscript, and providing cartoon pictures. This work is supported by the NSF under grants ATM 05-36921 and ATM 05-48952 and by NASA under grant NNG 04GG21G.

REFERENCES

Ambastha, A., Hagyard, M. J., & West, E. A. 1993, Sol. Phys., 148, 277
Antiochos, S. K. 1998, ApJ, 502, L181
Antiochos, S. K., DeVore, C. R., & Klimchuk, J. A. 1999, ApJ, 510, 485
Cameron, R., & Sammis, I. 1999, ApJ, 525, L61
Chen, J., Wang, H., Zirin, H., & Ai, G. 1994, Sol. Phys., 154, 261
Chen, W., Liu, C., & Wang, H. 2006, ApJ, submitted
Deng, N., Liu, C., Yang, G., Wang, H., & Denker, C. 2005, ApJ, 623, 1195
Deng, N., Xu, Y., Yang, G., Liu, C., Rimmele, T. R., Wang, H., & Denker, C. 2006, ApJ, 644, 1278
Falconer, D. A., Moore, R. L., & Gary, G. A. 2003, J. Geophys. Res., 108, SSH11
Gallagher, P. T., Moon, Y. J., & Wang, H. 2002, Sol. Phys., 209, 171
Hagyard et al. 1999, Sol. Phys., 184, 133
Hudson, H. S. 2000, ApJ, 531, L75
Ji, H., Huang, G., Wang, H., Zhou, T., Li, Y., Zhang, Y. & Song, M. 2006, ApJ, 636, L173
Ji, H., Wang, H., Goode, P. R., Jiang, Y., & Yurchyshyn, V. 2004a, ApJ, 607, L55
Ji, H., Wang, H., Schmahl, E. J., Qiu, J., & Zhang, Y. 2004b, ApJ, 605, 938
Jing, J., Song, H., Abramenko, V., Tan, C. & Wang, H. 2006, ApJ, 644, 1273
Kopp, R. A., & Pneuman, G. W. 1976, Sol. Phys., 50, 85
Kosovichev, A. G., & Zharkova, V. V. 2001, ApJ, 550, L105
Li, H., Sakurai, T., Ichimoto, K., & UeNo, S. 2000a, PASJ, 52, 465
———. 2000b, PASJ, 52, 483
Liu, C., Deng, N., Liu, Y., Falconer, D., Goode, P. R., Denker, C., & Wang, H. 2005, ApJ, 622, 722
Manoharan, P. K., van Driel-Gesztelyi, L., Pick, M., & Demoulin, P. 1996, ApJ, 468, L73
Melrose, D. B. 1997, ApJ, 486, 521
Moore, R. L., Sterling, A. C., Hudson, H. S., & Lemen, J. 2001, ApJ, 552, 833
Prasad, C. B. 2000, Ap&SS, 274, 463
Qiu, J., & Gary, D. E. 2003, ApJ, 599, 615
Song, H., Yurchyshyn, V., Yang, G., Tan, C., Chen, & Wang, H. 2006, Sol. Phys., in press
Spirock, T. J., Yurchyshyn, V. B., & Wang, H. 2002, ApJ, 572, 1072
Stoltz, J. 2005, M.S. thesis, New Jersey Inst. Technol.
Sudol, J. J., & Harvey, J. W. 2005, ApJ, 635, 647
Tang, F., & Moore, R. L. 1982, Sol. Phys., 77, 263
Veronig, A. M., Karlicky, M., Vrsnak, B., Temmer, M., Magdalenic, J., Dennis, B. R., Otruba, W., & Potzi, W. 2006, A&A, 446, 675
Wang, H., Ewell, M. W., Zirin, H., & Ai, G. 1994, ApJ, 424, 436
Wang, H., Gallagher, P., Yurchyshyn, V., Yang, G., & Goode, P. R. 2002a, ApJ, 569, 1026
Wang, H., Liu, C., Qiu, J., Deng, N., Goode, P. R., & Denker, C. 2004a, ApJ, 601, L195
Wang, H., Liu, C., Zhang, H., & Deng, Y. 2005, ApJ, 627, 1031
Wang, H., Qiu, J., Jing, J., Spirock, T. J., & Yurchyshyn, V. 2004b, ApJ, 605, 931
Wang, H., Song, H., Jing, J., Yurchyshyn, V., Deng, Y., Zhang, H., Falconer, D., & Jing, L. 2006, Chinese J. Astron. Astrophys., 6, 477
Wang, H., Spirock, T. J., Qiu, J., Ji, H., Yurchyshyn, V., Moon, Y. J., Denker, C., & Goode, P. R. 2002b, ApJ, 576, 497
Wang, H., Varsik, J., Zirin, H., Canfield, R. C., Leka, K. D., & Wang, J. 1992, Sol. Phys., 142, 11
Yurchyshyn, V., Karlicky, M., Hu Q., & Wang, H. 2006, Sol. Phys., 235, 147
Yurchyshyn, V. B., Wang, H., Abramenko, V., Spirock, T. J., & Krucker, S. 2004, ApJ, 605, 546
Zhang, H. 2001, ApJ, 557, L71
Zwaan, C. 1987, ARA&A, 25, 83